CFSTI PRICE(S) $ _____

Hard copy (HC) _____

Microfiche (MF) .50

ff 653 July 65

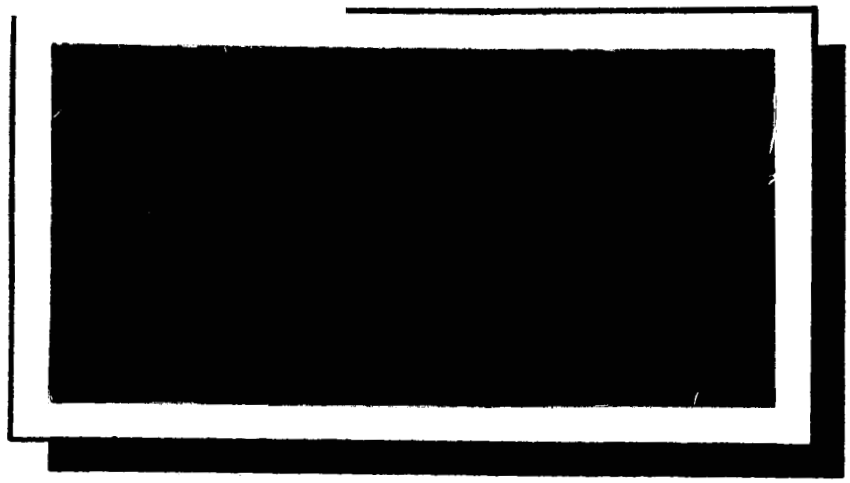

CENTER FOR SPACE RESEARCH
MASSACHUSETTS INSTITUTE OF TECHNOLOGY

CONTINUUM ELECTROMECHANICS GROUP

Traveling Wave Bulk Electroconvection Induced Across a Temperature Gradient

by
J.R. Melcher and M. S. Firebaugh

CSR TR-66-13
Oct. 28, 1966 NsG-368

TRAVELING WAVE BULK ELECTROCONVECTION INDUCED ACROSS A TEMPERATURE GRADIENT

by

James R. Melcher and Millard S. Firebaugh

Department of Electrical Engineering
Massachusetts Institute of Technology, Cambridge, Massachusetts

Summary

12924

If a temperature gradient is imposed on a slightly conducting liquid, a gradient in natural electrical conductivity generally results. It is shown that if the liquid is then subjected to a wave of electric field traveling perpendicular to the temperature and conductivity gradients, charges are induced in the liquid bulk. These charges relax to form a traveling wave which interacts with the imposed field to pump the liquid. The sign of the conductivity gradient determines whether the liquid is pumped in the same direction or a direction opposite to that of the traveling wave. Equations are given for the velocity profile in plane flow, showing the effect of fluid properties as well as of the frequency, wavelength, and potential of the traveling wave. Experiments support the significance of the theory. Observations of a type of bulk Rayleigh-Taylor instability are discussed.

Author

I. Introduction

Charges induced in a slightly conducting liquid through natural conduction processes can interact with a traveling wave of electric field to produce a fluid flow. One method of demonstrating this type of electroconvection is to introduce a potential wave traveling parallel to an air-liquid interface. Induced charges will relax through the liquid to the interface and form a traveling wave of surface charge which will lag the potential wave. An electric surface shear will result and the liquid will move.[1] In this kind of interaction the interface is a surface of singularity in the conductivity gradient. Because the conductivity is constant everywhere except at the interface, there are no free charges in the fluid bulk and hence no electric forces in the bulk.

An extension of this interaction results when the singular conductivity gradient is replaced by a continuous gradient. Then the interface can be eliminated by imbedding the electrodes carrying the traveling potential wave in a conduit boundary which makes mechanical (but not necessarily electrical) contact with the liquid. Charges are now induced in the bulk of the liquid. An internal wave of induced charge will travel along behind the traveling potential wave and the possibility for an electric force in the bulk of the liquid is created.

The electrical conductivity of slightly conducting liquids often depends strongly on the temperature.[2] Hence, if the walls of a conduit containing such a liquid are placed at different temperatures, the resulting temperature gradient within the enclosed liquid will be accompanied by a gradient in electrical conductivity. It is the bulk interaction of fluid with a traveling potential wave through the mechanism of a thermally induced gradient in electrical conductivity that is considered here.

A schematic representation of the physical situation is shown in Fig. 1. Plane flow between boundaries having the temperature difference $T_a - T_b$ is considered. The lower boundary is at the electric potential $\Phi = 0$, while electrodes imbedded in the upper boundary impose a traveling wave of potential with phases moving to the right. Because of the temperature difference, there is a variation in electrical conductivity across the channel. To prevent a Bénard[3] instability, T_a is greater than T_b. Many slightly conducting liquids have conductivities that increase with temperature.[2] Hence, as shown in Fig. 1, the electrical conductivity increases monotonically from the channel bottom to the top.

In Sec. II, a simple theory will be developed to predict the fluid flow resulting as the potential wave travels across the thermal gradient. Attention is confined to interactions where the effects of charge transport by the fluid are small and where the gradient in electrical conductivity is essentially constant across the channel. It is further assumed that the frequency of the traveling potential wave is large enough that the electromechanical effects occur through the time-average electric stresses. Similarly, the time required for thermal relaxation[4] is long compared to the period of the potential wave, so the temperature profile (and hence the property profile) of the fluid can be considered constant. These conditions

are met in many fluids. Experiments described in Sec. III illustrate the interaction and show that the theoretical model is meaningful even if the electrical conductivity varies by 80% across the channel.

Charges induced in the bulk of the fluid by the traveling potential wave lead to a transverse, as well as a longitudinal, force density. Because the liquid is heated from above, gravitational forces tend to stabilize the flow. However, this effect can be overcome by the transverse electrical forces and an electromechanical form of bulk Rayleigh-Taylor instability[5] produced. Experimental observations on this instability, made in Sec. III, indicate that it is somewhat related to forms of instability that have been reported.[6,7,8]

II Theoretical Model

Electric Potential Distribution

The ratio of a characteristic free charge relaxation time ε_c/σ_c to a time which characterizes the system dynamics is called the electric Reynolds number.[9] It is important to recognize that electrohydrodynamic induction interactions with a traveling potential wave involve two electric Reynolds numbers having quite different significances. First we can characterize the flow by the time ℓ_c/v_c, where ℓ_c and v_c are respectively a characteristic length and fluid velocity. Then the appropriate electric Reynolds number is $R_{e1} = \varepsilon_c v_c/\sigma_c \ell_c$. Second, we can use the period $2\pi/\omega$ of the imposed potential wave as a characteristic time to define the electric Reynolds number $R_{e2} = \varepsilon_c \omega/\sigma_c 2\pi$. In experiments designed to demonstrate traveling wave induction phenomena, R_{e2} is on the order of unity while R_{e1} is arbitrary. In the work described here, the

characteristic fluid velocity v_c is sufficiently small that R_{el} is at most 0.1. Hence, in the model developed in this section, we will take account of charge accumulation caused by the imposed time varying potential wave, but ignore the convection of charge.

Magnetic induction is negligible so the electric field $\bar{E}$ is irrotational

$$\bar{E} = -\nabla\Phi \tag{1}$$

Since the permittivity ε is nearly constant for the present considerations, the free-charge density q is given by

$$q = \varepsilon\nabla \cdot \bar{E} \tag{2}$$

Then, conservation of charge requires current density, $\bar{J}$, to be related to q by

$$\nabla \cdot \bar{J} + \frac{\partial q}{\partial t} = 0 \tag{3}$$

Two contributions to the current density can be important, one due to natural conduction and the other from convection of the charge q.

$$\bar{J} = \sigma\bar{E} + \bar{v}q \tag{4}$$

Because R_{el} is small, the second contribution to this equation will be ignored. Moreover, the conductivity, σ, will be assumed independent of $\bar{E}$ and q.

We will confine our attention to the time average effect on the fluid of the traveling potential wave. Hence, the flow is essentially steady and we assume that the temperature difference $T_a - T_b$ creates a distribution of electrical conductivity $\sigma(y)$ across the channel. This assumption is justified if the potential wave travels at a sufficiently high velocity that the fluid cannot respond to pulsations (of frequency ω/π) in the induced electric force density. Also, we assume that the electric field interaction does

not overcome the interaction of gravity with the thermally induced gradient in density to cause instability. Observations on this point are made in Sec. III.

The combination of Eqs. (1-4) (with $\bar{v}q = 0$ in Eq. (4)) gives an expression for the potential Φ.

$$\sigma \nabla^2\Phi + \nabla\sigma \cdot \nabla\Phi + \varepsilon\frac{\partial}{\partial t}\nabla^2\Phi = 0 \qquad (5)$$

If R_{el} were not small, there would be an additional term involving the velocity $\bar{v}$ of the fluid, and this equation could not be solved without recourse to the mechanical equations of motion. The approximation makes it possible to find the potential Φ from Eq. (5), then compute the time average electric stress and finally determine the resulting flow. According to the model used here, the fluid flow does not in turn distort the potential distribution.

If the variation of σ across the channel is monotonic, a reasonable approximation to Eq. (5) results if an average value of the conductivity, σ_o, is used as the coefficient of the first term, while $\nabla\sigma$ is approximated by $(\sigma_1/d)\,\bar{i}_y$. Here σ_1 is $\sigma(d) - \sigma(0)$, as shown in Fig. 1. Equation (5) becomes

$$\sigma_o\nabla^2\Phi + \frac{\sigma_1}{d}\frac{\partial\Phi}{\partial y} + \varepsilon\frac{\partial}{\partial t}\nabla^2\Phi = 0 \qquad (6)$$

On the upper surface of the channel, the potential has the traveling wave form

$$\Phi(x,d,t) = \mathrm{Re}\,\hat{V}\; e^{j(\omega t - k x)} \qquad (7)$$

Hence, the (x,t) dependence of the potential throughout the volume is assumed to have this same form, and it follows from Eq. (6) that

$$\frac{d^2\hat{\Phi}}{d\varsigma^2} + \frac{\eta}{(1+jS)}\frac{d\hat{\Phi}}{d\varsigma} - (kd)^2\,\hat{\Phi} = 0 \qquad (8)$$

where

$$\Phi = \mathrm{Re}\hat{\Phi}\ (y)\ \mathrm{exp}\,j(\omega t - kx)$$

$$\eta = \sigma_1/\sigma_o$$

$$S = \omega\varepsilon/\sigma_o$$

$$\zeta = y/d$$

The solution to Eq. (8) which satisfies the boundary condition of Eq. (7) and the condition that $\Phi = 0$ at the channel bottom is

$$\hat{\Phi} = \hat{V}\ (e^{P_1\zeta} - e^{P_2\zeta})/\ (e^{P_1} - e^{P_2}) \tag{9}$$

where for later purposes it is convenient to define

$$P_{(1)}_{(2)} = \frac{1}{2}\ (-a \pm b) \tag{10}$$

$$a = a_r + ja_i = \eta/(1 + S^2) - j\eta S/(1 + S^2) \tag{11}$$

$$b = b_r + jb_i = A\cos\left(\frac{\theta}{2}\right) - jA\sin\left(\frac{\theta}{2}\right) \tag{12}$$

where

$$A = \left\{[4(kd)^2 + \frac{\eta^2(1 - S^2)}{(1 + S^2)}2]^2 + [\frac{2\eta^2 S}{(1+S^2)^2}]^2\right\}^{\frac{1}{4}}$$

$$\theta = \tan^{-1}\left\{[2\eta^2 S/(1+S^2)^2]/\ [4(kd)^2 + \eta^2(1-S^2)/\ (1+S^2)^2]\right\}$$

Equation (9) and the subsequent definition of variables is the desired solution for the electric potential.

Electric Stress

For the present purposes, there is no gradient of the pressure along the channel. (In experiments to be described in Sec. III the channel will be re-entrant.) Hence, it is convenient to compute the electric shear stress rather than the force density throughout the volume. The electric shear stress acting in the x direction is[10]

$$T^e_{xy} = \varepsilon E_x E_y \tag{13}$$

with a time average value of

$$\langle T^e_{xy} \rangle = \frac{\varepsilon}{2} \mathrm{Re}\ \hat{E}_x \hat{E}^*_y$$

where * indicates the complex conjugate. Here, a complex electric field amplitude has been defined such that $\bar{E} = \mathrm{Re}\ \hat{\bar{E}}(y) \exp j(\omega t - kx)$. From Eq. (9)

$$\hat{\bar{E}} = \frac{\hat{V}}{d(e^{P_1} - e^{P_2})} \left[jkd(e^{P_1\zeta} - e^{P_2\zeta})\bar{i}_x - (p_1 e^{P_1\zeta} - p_2 e^{P_2\zeta})\bar{i}_y \right] \quad (15)$$

It is possible, by means of considerable manipulation, to use these expressions together with the definitions of Eqs. (10-12) to write Eq. (14) as

$$\langle T^e_{xy} \rangle = D\, f(\zeta) \quad (16)$$

where

$$f(\zeta) = e^{-a_r(\zeta-1)} [b_r \sin b_i\zeta - b_i \sinh b_r\zeta + a_i(\cosh b_r\zeta - \cos b_i\zeta)]$$

$$D = \varepsilon k \hat{V}\hat{V}^* / [4d(\cosh b_r - \cos b_i)]$$

The distribution of shear stress given by Eq. (16) will now be used to compute the velocity profile.

Velocity Distribution

Because the channel is re-entrant, there is no variation of pressure in the x direction. The conditions of plane steady flow imply that momentum does not make a contribution to the force balance. There remains the viscous forces to be balanced by the induced electric forces. There are no variations of the time average electric force with the x direction. It is therefore necessary that the sum of the electric and viscous shear stresses be independent of the depth (y). That is, force equilibrium requires that

$$\frac{\mu}{d} \frac{dv_x}{d\zeta} + \langle T^e_{xy} \rangle = C$$

where C is a constant and the viscosity μ is a function of depth (because of the temperature difference between the top and bottom of the channel.) The velocity profile follows from an integration of Eq. (17). The resulting constant of integration and C are used to satisfy the conditions that $v_x(\zeta = 0) = v_x(\zeta = 1) = 0$. Then, incorporation of Eq. (16) gives the velocity profile

$$v_x = Dd\left[F\int_0^{\zeta}\frac{d\xi}{\mu(\zeta)} - \int_0^{\zeta}\frac{f(\zeta)d\zeta}{\mu(\zeta)}\right] \tag{18}$$

where $F = \int_0^1 \frac{f(\zeta)}{\mu(\zeta)}\,d\zeta \Big/ \int_0^1 \frac{d\zeta}{\mu(\zeta)}$

The integrals of Eq. (18) are most easily evaluated numerically.

The Pumping Mechanism

The essential features of the velocity profile, as it depends on the traveling wave frequency and physical parameters, can be illustrated in the limiting case where μ is constant and

$$1 >> 2kd >> \eta \tag{19}$$

The latter condition requires that the wavelength be much longer than the transverse dimension d, and that the gradient in conductivity be small, in which case Eq. (16) reduces to

$$Df(\zeta) = \frac{-\eta S\zeta^2 \epsilon k V^2}{4(1+S^2)d} \tag{20}$$

Now, if μ is taken as constant, Eq. (18) can be evaluated as

$$v_x = \frac{-\eta S\epsilon k V^2}{12(1+S^2)\mu}\,(\zeta - \zeta^3) \tag{21}$$

The most interesting feature of this expression is its sign. If the electrical conductivity has a positive gradient ($\eta > 0$),

flow occurs in a direction opposite to that of the traveling potential wave. This contrasts with magnetohydrodynamic induction interactions,[11] and can be understood with the help of Fig. 2.

Suppose that the frequency ω is very low. Then, the current density J_y of Fig. 2a is related to E_y by

$$E_y = \frac{J_y}{\sigma} \tag{22}$$

where, because the frequency is low, the conduction current must be essentially independent of y. Hence, for long wavelengths

$$q \cong \varepsilon \frac{dE_y}{dy} = \frac{-\varepsilon J_y}{\sigma^2} \frac{d\sigma}{dy} \tag{23}$$

so that a positive gradient in electrical conductivity will lead to a negative volume charge density. At a frequency such that $S \approx 1$, these induced charges relax to the fluid volume with a spatial phase which lags that of the surface charges on the electrodes, as shown in Fig. 2b. The sign of the volume charge, determined by the positive conductivity gradient, is such that the fluid is repelled in the direction opposite to that of the wave.

In fact, it can be shown from Eqs. (2) (9) and (10) that if the surface charge on the electrode at $\xi = 1$ is $\mathrm{Re}\hat{\sigma}_s \exp j(\omega t - kx)$ then the volume charge just below the electrode is

$$q(\xi = 1) = \mathrm{Re}\hat{\sigma}_s \eta e^{j(\omega t - kx)} (1 - jS)/[(1+S^2)d] \tag{24}$$

which makes apparent the dependence of the lag in spatial phase on the normalized frequency S. When S = 1, the phase lag is 45°, as shown in Fig. 2b. This is also the frequency at which the largest fluid velocity is obtained, as can be seen from Eq. (21). In a way which is characteristic of induction processes,[1] the velocity approaches zero as S is made large or small.

From Eq. (21) it is also seen that the velocity profile is skewed upward, with the point of maximum velocity occurring at $\zeta = 1/\sqrt{3}$, where the velocity is, from Eq. (21)

$$v_{peak} = -\eta S \epsilon k V^2 / [(1+S^2)\mu 18\sqrt{3}] \qquad (25)$$

The velocity is higher near the upper electrodes, because it is these electrodes rather than the equipotential channel bottom which produce the electrical shear on the fluid.

III Experimental Observations

Apparatus and Parameters

The thermally induced electroconvection was studied in the apparatus shown in Fig. 3. The fluid (in this case corn oil), was contained in the annulus between plexiglass cylinders sealed to an aluminum bottom plate which rested in ice water. A metallic structure then formed the bottom of the channel by making thermal contact with the bottom plate. Segmented electrodes were sealed to the lower surface of an upper region containing hot oil, to provide the channel top. The traveling potential wave was produced by a commutator mechanism,[1] not shown in Fig. 3, electrically connected to the segments.

Three thermometers, located in the insulating channel wall, were used to determine an approximate linear temperature profile. The electrical conductivity and viscosity profiles were then inferred from conventional measurements taken over an appropriate range of temperatures. Figures 4 and 5 show the variation of these parameters with temperature, with the channel top and bottom assuming the temperatures shown. The broken lines indicate the approximate linear variations assumed in evaluating the parameters σ_o and σ_1 and for the numerical integration of Eq. (18). As may be seen from Fig. 4, a modest

temperature difference leads to a significant variation in electrical conductivity ($\eta \approx 1$). In fact, the variation is large enough that approximations introduced with Eq. (6) are a possible source of discrepancies between theory and experiment, although not the cause of much difficulty here. A discussion of how the theory can be generalized to an arbitrary conductivity profile will be given in Sec. IV.

In the experiment, the mean channel length (0.88 m) constituted one wavelength. The corresponding wavenumber and other physical parameters were as shown in Table 1.

Velocity Measurements

The normalized electric shear stress $f(\zeta)$ (Eq. 16), based on the parameters of Table 1, is as shown in Fig. 6. Here, the peak potential has been taken as 8.25 kV. This corresponds to an experimental peak potential of 12.5kV, since the potential wave produced by the commutator mechanism[1] was not a purely sinusoidal function of time. The velocity profile shown in Fig. 6 is the result of a numerical integration of Eq. (18).

To observe the fluid motion, one section of the channel was constructed with side walls made of parallel glass plates. This made it possible to project light through the flow and observe fluid motions illuminated either by a point source or by a Schlieren system. The magnification was sufficient that small particles of dust entrained in the flow could be used to measure the fluid velocity.

The dependence of the absolute peak velocity on the frequency of the imposed potential wave is shown in Fig. 7. The solid line is predicted by Eq. (18). Flow was observed in a direction opposite to that of the traveling wave. At the low end of this plot, the flow velocity displayed an appreciable periodicity at twice the frequency of the imposed traveling wave.

Each measurement shown in Fig. 7 represents the average value of the flow velocity.

According to Eq. (18), at a given frequency the fluid velocity is a linear function of the imposed potential amplitude squared. With a frequency $\omega/2\pi = 0.4$ cps, the peak velocity was found to be as shown in Fig. 8, where the solid line indicates the prediction of Eq. (18). Brackets on a data point indicate the extremes of five measurements.

The major sources of error in predicting the flow velocity appear to be due to: a) property measurements (especially the electrical conductivity which essentially determines the frequency at which the peak appears in Fig. 7), b) the finite width of the channel (5.4 cm compared to a depth d of 3 cm.), c) the theoretical approximation of the conductivity and its transverse gradient as having constant average values, and d) effects from the time variation in the electric stress.

Instability

One of the most important limitations on the range of traveling wave potentials and frequencies that can be used results from flow instability. As the traveling wave frequency is reduced, with the peak potential maintained constant, a point is reached where the potential is responsible for instability, rather than inducing a steady flow. This instability appears as a complete disruption of the flow pattern, with an ensuing turbulent motion that drastically alters the thermal gradient.

Fig. 9 shows a Schlieren projection of the channel. The electrode segments are evident at the top of the pictures, with the channel bottom just out of view below. The potential wave travels to the right, while in Fig. 9a the fluid moves steadily to the left. A region of given thermal gradient is indicated

by the dark band. (The periodic appearance of this band is due to the electrode segments rather than to the spatial periodicity of the traveling potential wave which had a wavelength 40 times the segment length). Fig. 9b shows the effect of reducing the traveling wave frequency. The mean flow was essentially destroyed, with an accompanying disruption of the temperature distribution. If the frequency was again raised, the flow immediately assumed a stable steady character, as shown in Fig. 9c. However, a considerable length of time was required for the temperature profile to return to that obtained originally (Fig. 9a) because of the long thermal relaxation time for the liquid.

The instability appeared to have little to do with the flow. It seemed related to the accumulation of free charges in the fluid bulk and the accompanying transverse electric force distribution. At lower peak potentials, flow stability was retained at lower frequencies. But, as the peak potential was raised, the lowest frequency for stable flow was also increased.

Instability appeared to be of the bulk Rayleigh-Taylor form[5] with incipience dependent on the competing stabilizing effects of gravity and destabilizing effects of the electric field. Complicating features were the electrical (and possibly thermal) relaxation processes, the effects of viscosity on the growth rate, and the temporal periodicity of the driving potential. Investigations in this regard will be reported.

IV Conclusion and Further Observations

The experiments described in Sec. III, together with other qualitative observations, indicate that the simple theory of Sec. II is an appropriate description of the flow that results when a potential wave travels perpendicular to a thermally

induced gradient in electrical conductivity. The theoretical model is limited to situations where the conductivity and its gradient can be represented by averages over the channel profile. This approach can be refined in a straightforward way by dividing the flow into regions, each of which is represented by an appropriate σ_o and σ_1, as shown in Fig. 10. Then, solutions for the electric potential are spliced together by the boundary conditions. This approach is necessary if the conductivity distribution is not monotonic, as shown in Fig. 10b. The electric shears on the fluid are then opposed in the upper and lower regions. For the case shown in Fig. 10b, at least two regions would be required to predict the velocity profile.

Qualitative experimental observations have been made where the conductivity profile was essentially as sketched in Fig. 10b. In these cases, the fluid was inhomogeneous, in addition to being subjected to a temperature gradient. With a slightly conducting fluid on top (mineral oil), the conductivity gradient was negative in the upper region due to the inhomogeneity, but positive in the lower region due to the thermal gradient. (The lower fluid was corn oil, which has a conductivity much larger than that of the mineral oil.) Flow resulted in either direction or simultaneously in opposite directions, depending on the frequency of the traveling potential wave. These results are as would be expected from the simple model of Sec. II. They illustrate the point that the distributed gradient in electrical conductivity could as well be produced by using equitemperature layers of fluid having differing electrical conductivities. As emphasized in the introduction, there is a close connection between the mechanism for bulk pumping described here and for the surface pumping that has been reported.[1] The surface pumping can also be demonstrated with the conductivity profile such that the fluid moves in a direction opposite to that of the traveling

wave.[12] This has been demonstrated experimentally by arranging the electrodes so that a layer of fluid having a free surface was exposed from below to the traveling potential wave. If the electrodes were placed below the channel rather than above, as described in Sec. III, a fluid supporting a positive conductivity gradient would be pumped in the same direction as the traveling field.

It appears that the bulk interaction described here has application to situations where very slightly conducting liquids must be pumped through an electrically insulating conduit. From a basic point of view, it constitutes one of many mechanisms by which slightly conducting fluids can be motivated by an electric field.

Acknowledgments:

The suggestions of Mr. Edmund Devitt and experimental assistance of Mr. David Assael were valuable in completing this work, which was supported by NASA Research Grant NsG-368.

References

1. J. R. Melcher, Phys. Fluids 9, 1543 (1966).
2. A. E. Knowlton, Standard Handbook for Electrical Engineers, (McGraw-Hill Book Co. Inc., New York, N.Y., 1957), p.410.
3. S. Chandrasekhar, Hydrodynamic and Hydromagnetic Stability Oxford Press, London, 1961), p. 9.
4. W. M. Rohsenow and H.Y. Choi, Heat, Mass, and Momentum Transfer (Prentice-Hall, Inc., Englewood Cliffs, New Jersey, 1961) p. 110.
5. Lord Rayleigh, Scientific Papers (Dover Pub. Inc., 1964), Vol. II, p. 200.
6. D. Avsec and M. Luntz, Comp. rend. 204, 757 (1937).
7. G. A. Ostroumov, Soviet Phys. J.E.T.P., 2, 428 (1956).
8. W.V.R. Malkus and G. Veronis, Phys. Fluids, 4, 13 (1961).
9. O. M. Stuetzer, Phys. Fluids, 5, 534, (1962).
10. J. A. Stratton, Electromagnetic Theory (McGraw-Hill Book Co., Inc., 1941), p. 147.
11. L. P. Harris, Hydromagnetic Channel Flows (M.I.T. Press, Cambridge, Massachusetts, 1960), 61.
12. M. S. Firebaugh, M.S. thesis, Massachusetts Institute of Technology (1966).

Tables

Table 1 Parameters for experiment using corn oil as fluid

$\sigma_o = 6.9 \times 10^{-11}$ mhos/m	$\mu = (7.7\text{-}5.25) \times 10^{-2}$ kg/m sec.
$\sigma_1 = 7.9 \times 10^{-11}$ m hos/m	$d = 3 \times 10^{-2}$ m
$\varepsilon = 3.1\ \varepsilon_o$	$k = 7.08\ m^{-1}$

LIST OF FIGURE TITLES

Fig. 1. A slightly conducting fluid flows in the x (or -x) direction between plane parallel walls having the temperature difference $T_a - T_b (T_a > T_b)$. A traveling potential wave is imposed by means of electrodes in the upper boundary. Because of thermally induced gradients in the conductivity $\sigma(y)$, free charges are induced in the fluid bulk. For the case shown, the fluid moves in a direction opposite to that of the traveling wave. $[\omega/k > 0, v_x < 0]$

Fig. 2. Cross-sectional view of plane flow, showing traveling wave imposed above the fluid and constant potential plane below the fluid. a) With a positive gradient in electrical conductivity, a positive conduction current leads to a negative volume free charge. b) With the traveling wave of potential, charges relax to the volume where they lag the charges induced on the electrodes by the imposed potential. The sign of the volume charge, determined by the conductivity gradient, is such that the fluid is repelled in the direction opposite to that of the wave.

Fig. 3. Cross-sectional and top view of channel. The channel bottom makes thermal contact with ice water, while the upper electrodes are heated by circulating hot oil. The temperature profile is measured by means of three thermometers in the plexiglass side wall.

Fig. 4. Electrical conductivity as a function of temperature for the corn oil used in the experiment of Fig. 3. With the temperature profile essentially linear, the top and bottom assume the temperatures shown. The broken line indicates approximate linear relation used in theory.

List of Figures (cont.)

Fig. 5. Viscosity of corn oil as a function of temperature. The top and bottom assume temperatures as indicated. The broken line was used for the theoretical relations.

Fig. 6. Fluid velocity and normalized electric shear stress as a function of normalized transverse position $\zeta = y/d$.

Fig. 7. Absolute peak velocity as a function of frequency. The solid curve is predicted by numerical integration of Eq. (18).

Fig. 8. Absolute peak velocity at $\omega/2\pi = 0.4$ as a function of the square of the peak traveling wave potential. The solid line is predicted by numerical integration of Eq. (18).

Fig. 9. Schlieren photograph of fluid viewed as shown in Fig. 3. a) Flow to left established initially by turning up potential with $\omega/2\pi \cong 0.4$. b) Instability destroys velocity profile as $\omega/2\pi$ is reduced to <0.1 cps. at constant potential. c) Flow reestablished with altered temperature profile as frequency is raised. The distance between vertical lines is 1 cm.

Fig. 10 The approach taken in Sec. II can be refined to account for large variations in conductivity by dividing the flow into regions. Solutions are spliced together between regions by the boundary conditions. a) Two regions defined so that σ_o is an improved average of σ over the appropriate region of flow. b) Inversions of the σ profile require a multi-region approach, since induced electric forces differ in direction over profile.

Fig. 1. A slightly conducting fluid flows in the x (or -x) direction between plane parallel walls having the temperature difference $T_a - T_b (T_a > T_b)$. A traveling potential wave is imposed by means of electrodes in the upper boundary.

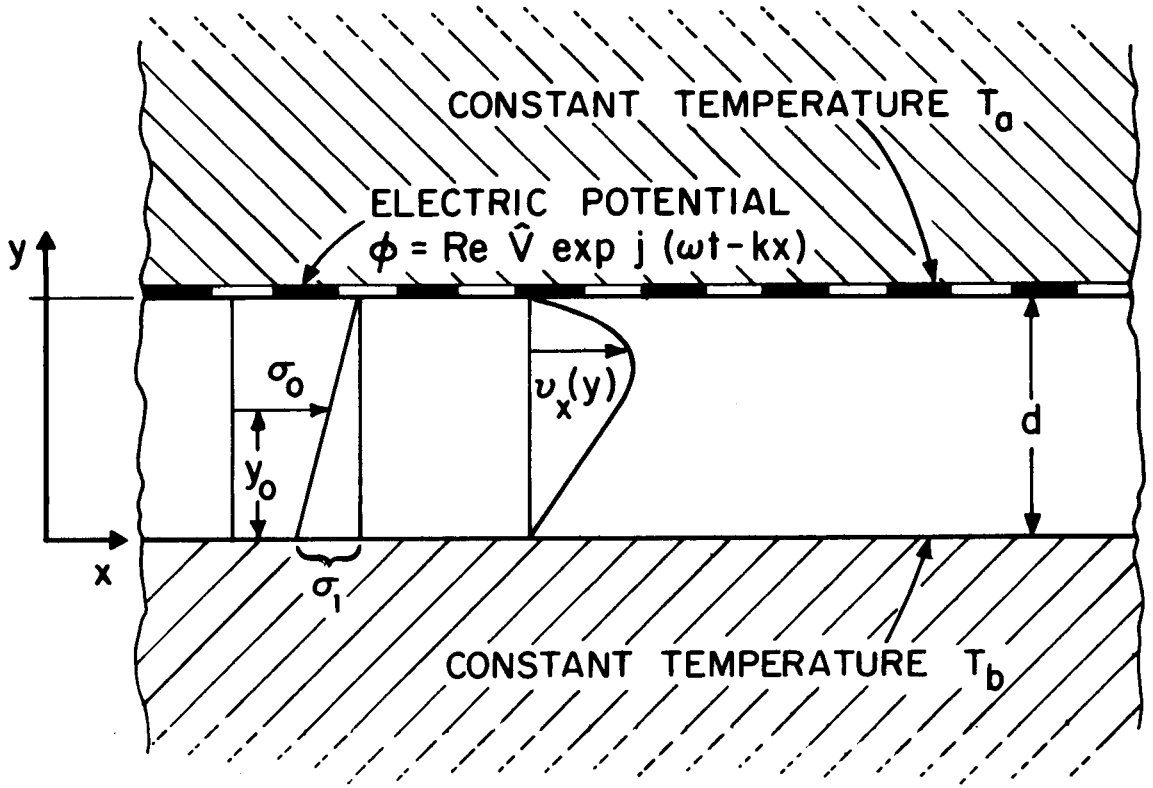

Because of thermally induced gradients in the conductivity $\sigma(y)$, free charges are induced in the fluid bulk. For the case shown, the fluid moves in a direction opposite to that of the traveling wave. [$\omega/k > 0$, $v_x < 0$]

Fig. 2. Cross-sectional view of plane flow, showing traveling wave imposed above the fluid and constant potential plane below the fluid. a) With a positive gradient in electrical conductivity, a positive conduction current leads to a negative volume free charge. b) With the traveling wave

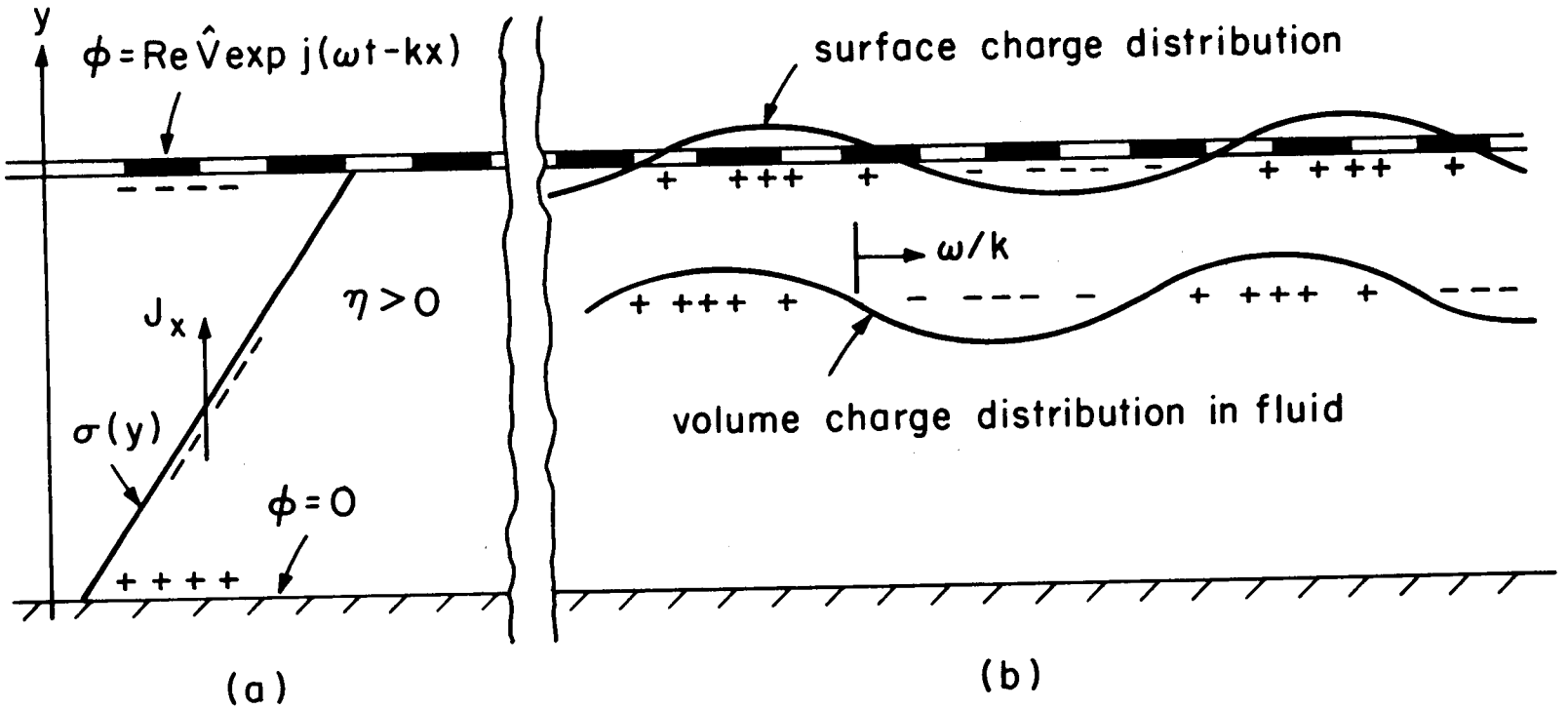

of potential, charges relax to the volume where they lag the charges induced on the electrodes by the imposed potential. The sign of the volume charge, determined by the conductivity gradient, is such that the fluid is repelled in the direction opposite to that of the wave.

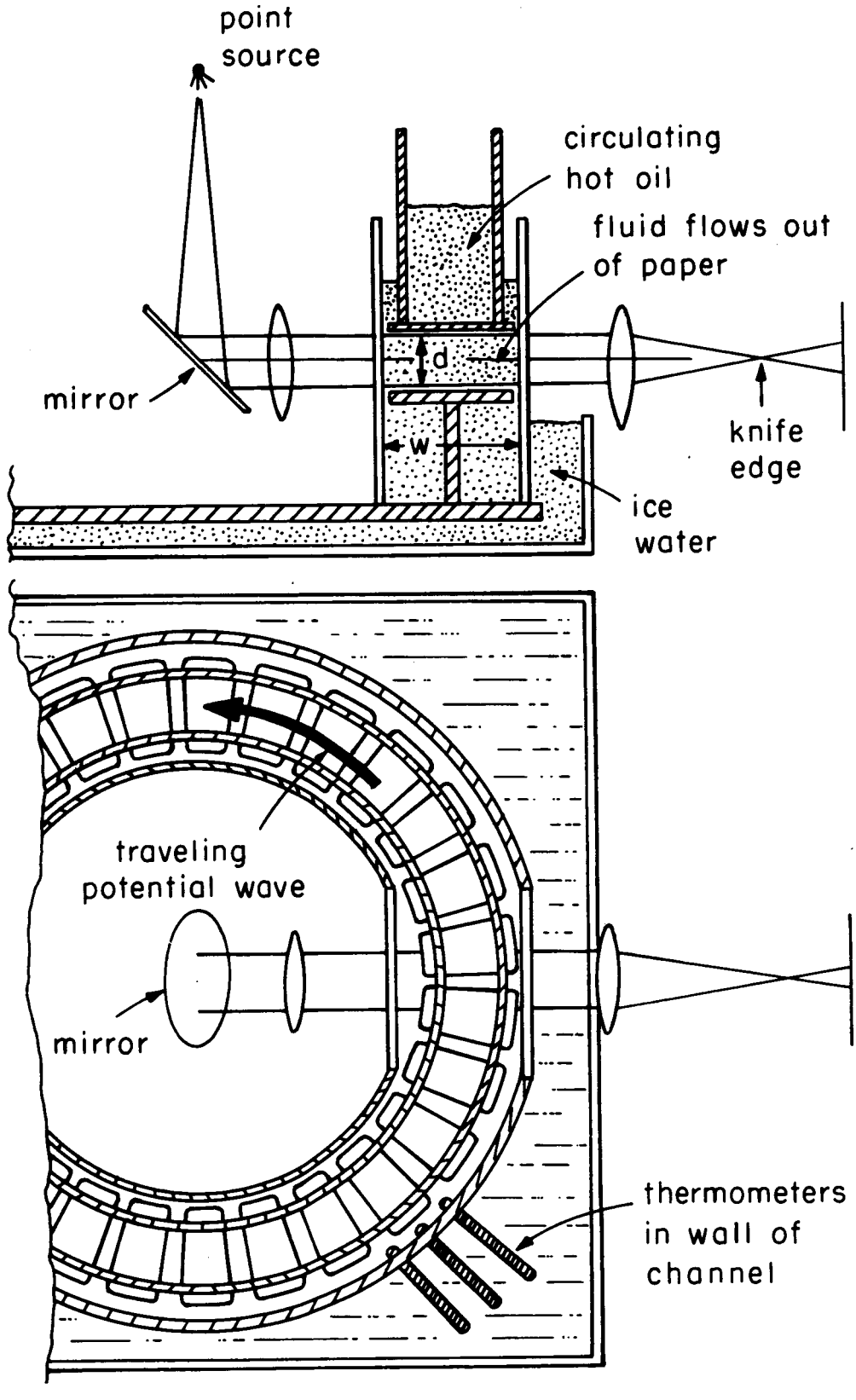

Fig. 3. Cross-sectional and top view of channel. The channel bottom makes thermal contact with ice water, while the upper electrodes are heated by circulating hot oil. The temperature profile is measured by means of three thermometers in the plexiglass side wall.

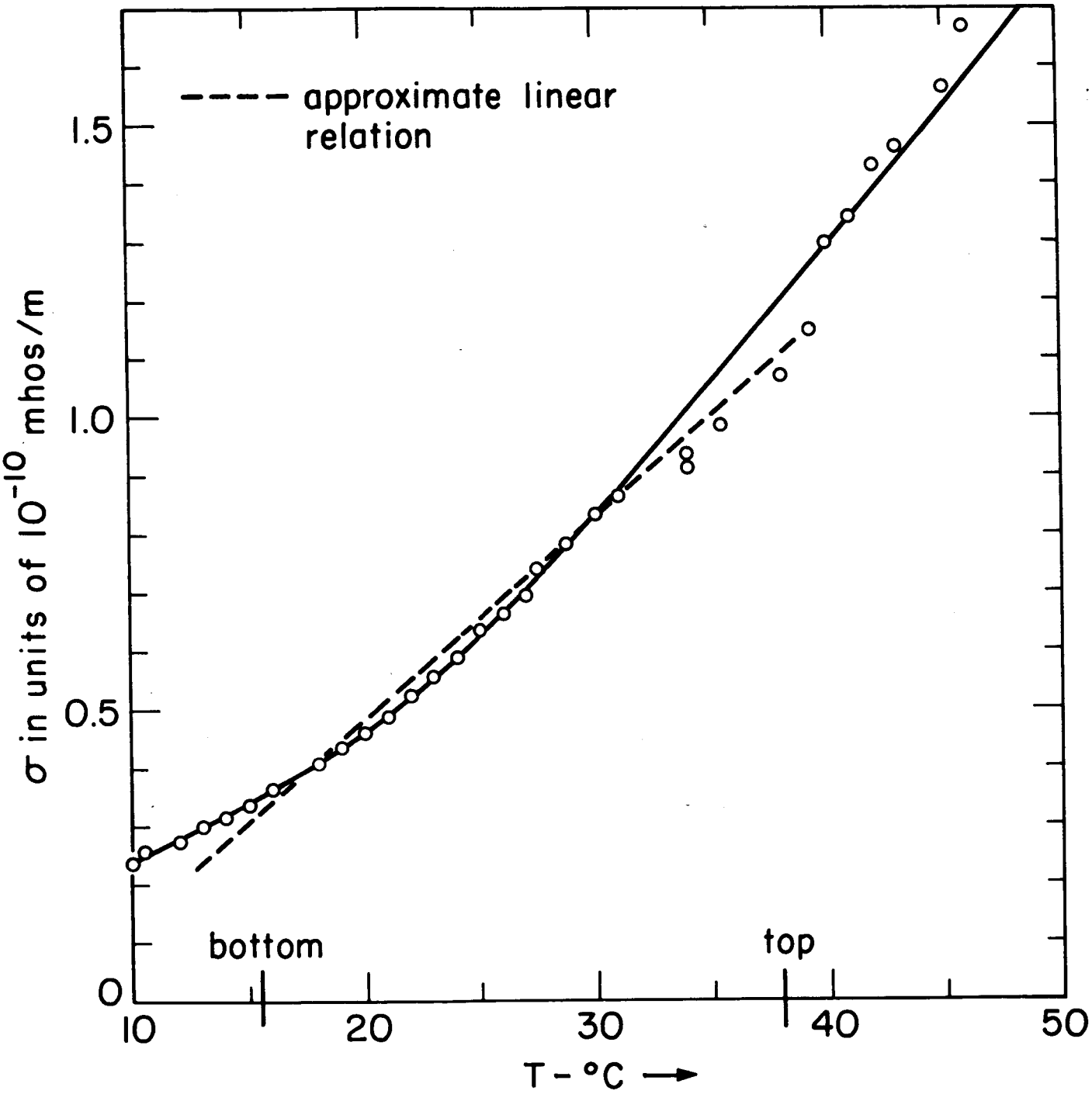

Fig. 4. Electrical conductivity as a function of temperature for the corn oil used in the experiment of Fig. 3. With the temperature profile essentially linear, the top and bottom assume the temperatures shown. The broken line indicates approximate linear relation used in theory.

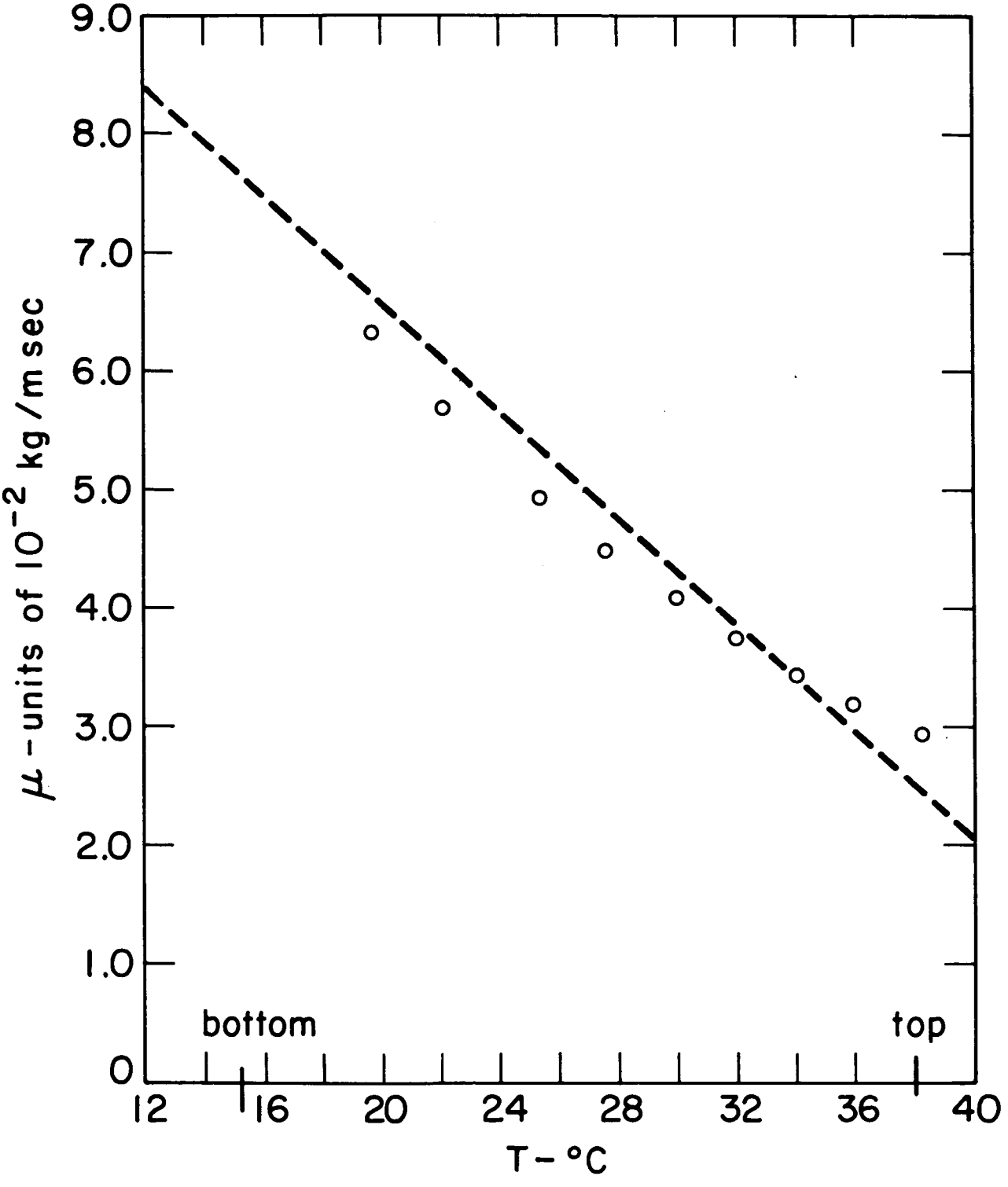

Fig. 5. Viscosity of corn oil as a function of temperature. The top and bottom assume temperatures as indicated. The broken line was used for the theoretical relations.

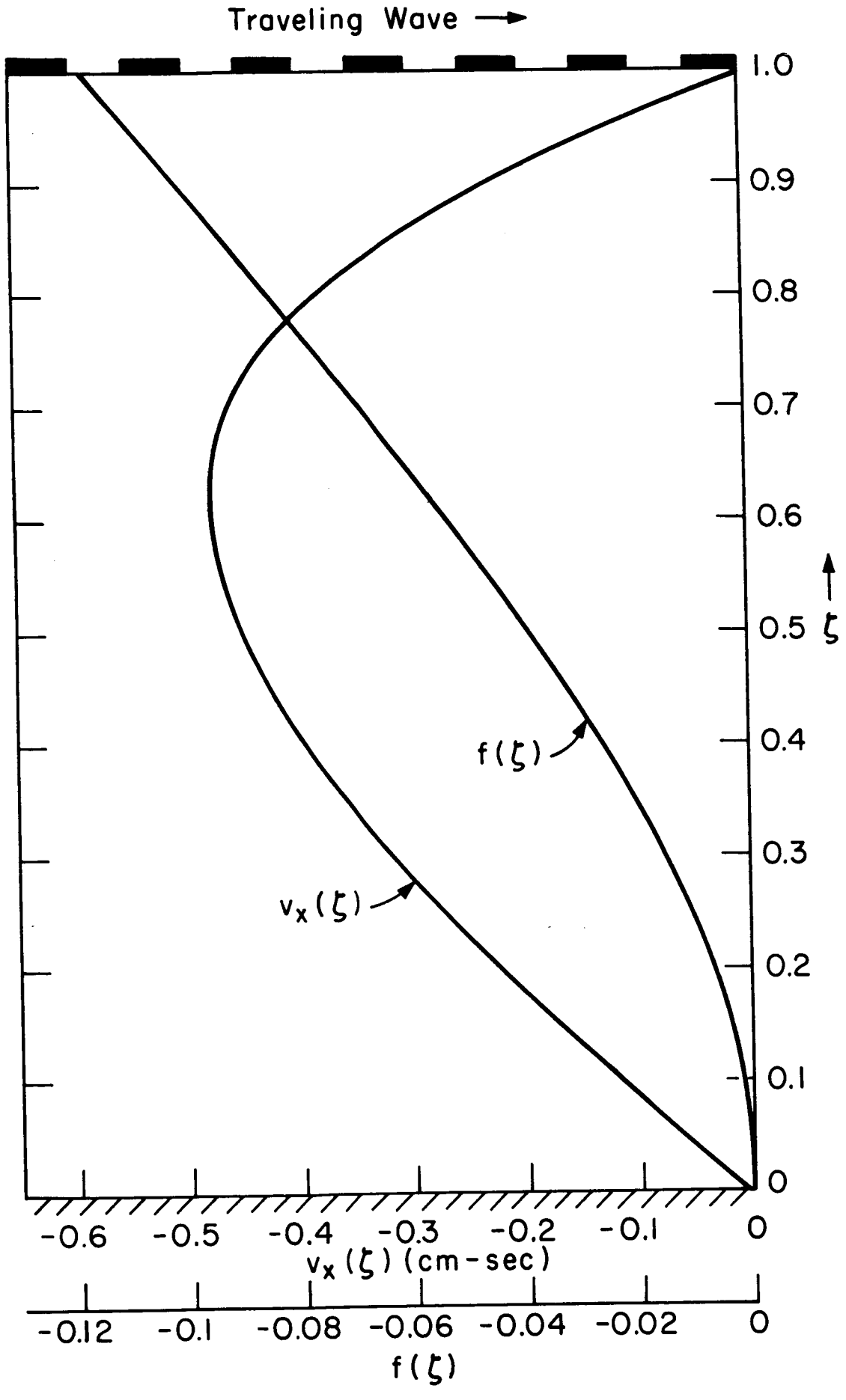

Fig. 6. Fluid velocity and normalized electric shear stress as a function of normalized transverse position $\zeta = y/d$.

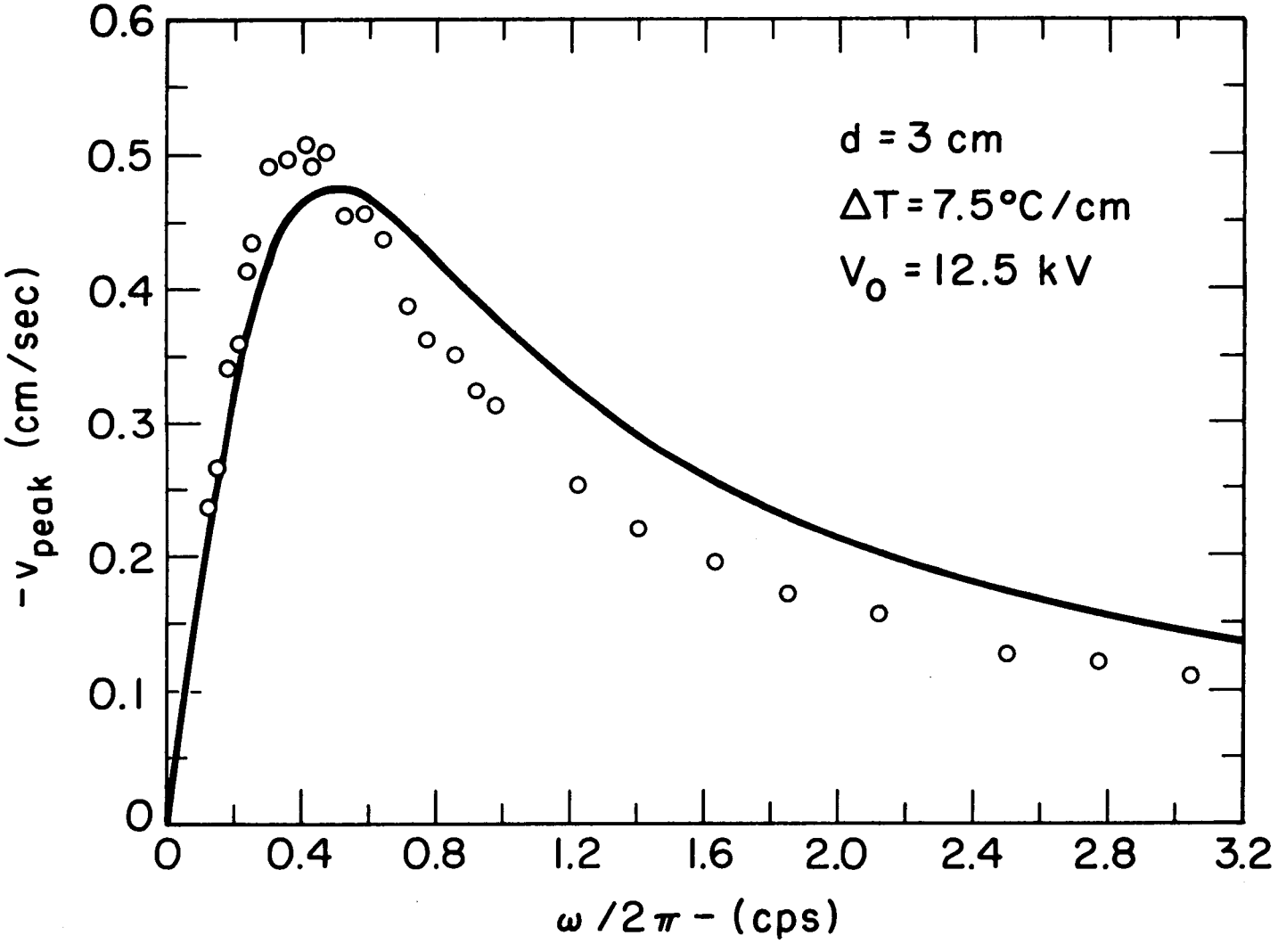

Fig. 7. Absolute peak velocity as a function of frequency. The solid curve is predicted by numerical integration of Eq. (13).

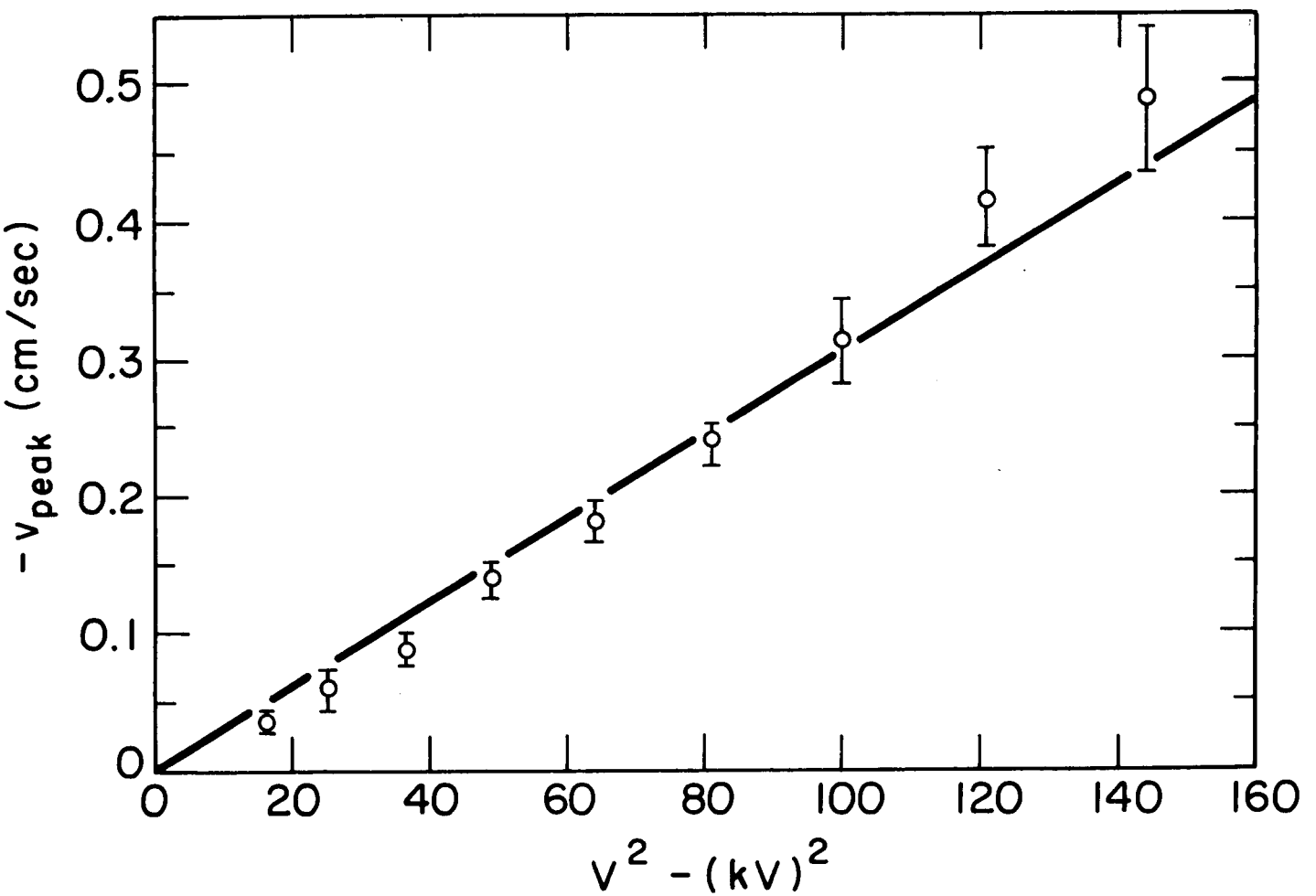

Fig. 3. Absolute peak velocity at $\omega/2\pi = 0.4$ as a function of the square of the peak traveling wave potential. The solid line is predicted by numerical integration of Eq. (18).

Fig. 9. Schlieren photograph of fluid viewed as shown in Fig. 3. a) Flow to left established initially by turning up potential with $\omega/2\pi \cong 0.4$. b) Instability destroys velocity profile as $\omega/2\pi$ is reduced to <0.1 cps. at constant potential. c) Flow reestablished with altered temperature profile as frequency is raised. The distance between vertical lines is 1 cm.

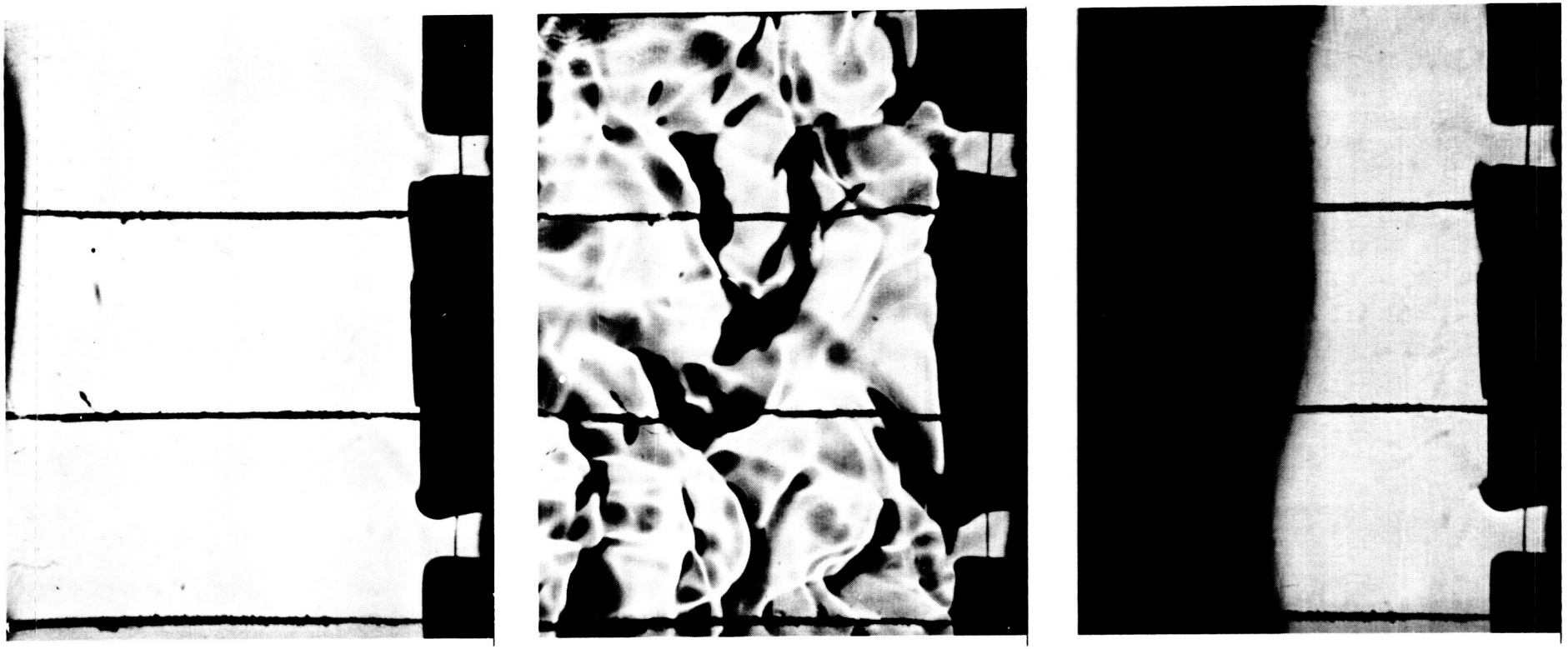

(c) (b) (a)

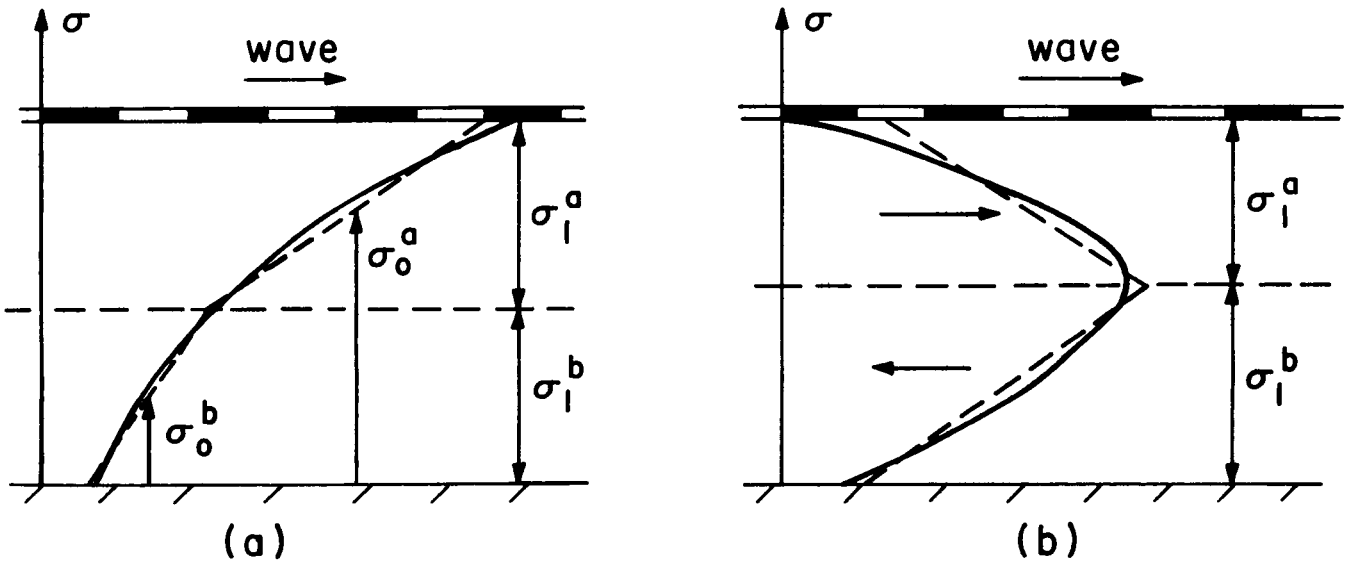

Fig. 10 The approach taken in Sec. II can be refined to account for large variations in conductivity by dividing the flow into regions. Solutions are spliced together between regions by the boundary conditions. a) Two regions defined so that σ_o is an improved average of σ over the appropriate region of flow. b) Inversions of the σ profile require a multi-region approach, since induced electric forces differ in direction over profile.